NASA TECHNICAL NOTE

NASA TN D-4428

c. 1

NASA TN D-4428

LOAN COPY: RETU
AFWL (WLIL-
KIRTLAND AFB, N

0131185

TECH LIBRARY KAFB, NM

EXPERIMENTAL MODES OF VIBRATION OF 14° CONICAL-FRUSTUM SHELLS WITH FREE ENDS

by John S. Mixson

Langley Research Center
Langley Station, Hampton, Va.

RECEIVED
4 APR 1968
Technical Library
AF Weapons
Laboratory

NATIONAL AERONAUTICS AND SPACE ADMINISTRATION • WASHINGTON, D. C. • APRIL 1968

TECH LIBRARY KAFB, NM

0131185

EXPERIMENTAL MODES OF VIBRATION OF 14° CONICAL-FRUSTUM SHELLS WITH FREE ENDS

By John S. Mixson

Langley Research Center
Langley Station, Hampton, Va.

NATIONAL AERONAUTICS AND SPACE ADMINISTRATION

For sale by the Clearinghouse for Federal Scientific and Technical Information
Springfield, Virginia 22151 – CFSTI price $3.00

EXPERIMENTAL MODES OF VIBRATION OF 14° CONICAL-FRUSTUM SHELLS WITH FREE ENDS*

By John S. Mixson
Langley Research Center

SUMMARY

In experimental studies of the vibrations of conical and cylindrical shells, some modes having different numbers of circumferential waves at different locations along the shell meridian have been obtained. (Such modes are termed "mixed modes" herein.) To investigate the occurrence of such modes, five conical-frustum shells were vibrated and their resonant frequencies and nodal patterns determined. The shells had a half-angle of 14° and three wall thicknesses. Three shells had butt-welded seams and two had lap-welded seams. The suspension-system stiffness was varied, and two types of excitation were used.

Experimentally determined frequencies and the location of the circumferential node line are shown to be in good agreement at low frequencies with values calculated by means of inextensional shell theory. Mixed modes occurred when the shell or test setup departed substantially from ideal conditions. Examples of nonideal conditions include imperfections or lap-welded seams on the shell, stiff suspension systems, and forced response of two modes at nearly the same frequency. It is shown that the experimental nodal patterns of these modes can be obtained by superposition of theoretical modes of an ideal conical shell.

INTRODUCTION

Conical-frustum shells are incorporated in most present-day launch vehicles as interstage sections or engine exhaust nozzles. The analytical techniques used for prediction of the response of these shells to the applied dynamic forces are relatively complex, and therefore often require verification by experiment. Such verification usually involves comparison between experimental and analytical frequencies and mode shapes.

*Some of the information presented herein was previously included in the paper "On the Modes of Vibration of Conical-Frustum Shells With Free Ends," presented at the 4th Aerospace Sciences Meeting, Los Angeles, California, June 27-29, 1966 (AIAA paper No. 66-450) and published in J. Spacecraft Rockets, vol. 4, no. 3, Mar. 1967, pp. 414-416.

In recent experimental studies of conical shells (refs. 1, 2, and 3) and cylindrical shells (ref. 4), some nodal patterns associated with resonant frequencies were found to be in disagreement with predictions of linear thin-shell theory. The nature of the disagreement is illustrated in figure 1, where nodal patterns of a free-edge conical-frustum shell are viewed from the small end of the cone. (The relative diameters of the ends have been changed to facilitate display of the nodal pattern.) The theoretical equations describing the vibrations of a shell of revolution have solutions that are sinusoidal in the circumferential coordinate (ref. 5). With such solutions the node lines of a normal mode of a conical shell lie along the meridian, as shown in figure 1(a). In contrast, the experimental nodal pattern, shown in figure 1(b), has curved node lines that in two cases form "loops" that intersect only the large end of the cone. It is proposed in reference 3 that the theory be modified to obtain agreement with the experimentally observed nodal patterns. On the other hand, it has been suggested that such experimental nodal patterns result from forced response of normal modes having nearly the same frequency (ref. 6) or from coupling of normal modes by lap-welded seams (ref. 4).

The investigation described herein was undertaken to clarify and demonstrate the causes of experimental nodal patterns such as those shown in figure 1(b). The resonant frequencies and nodal patterns of five conical-frustum shells were determined experimentally. The shells were of three thicknesses. Three shells had uniform thickness, one shell had a single lap-welded seam giving double thickness along a meridian, and one shell had three lap-welded seams. The shells were supported by a suspension system designed to simulate free-boundary conditions at both ends of the shell. The stiffness of the suspension system was varied and its effect on the frequencies and nodal patterns was

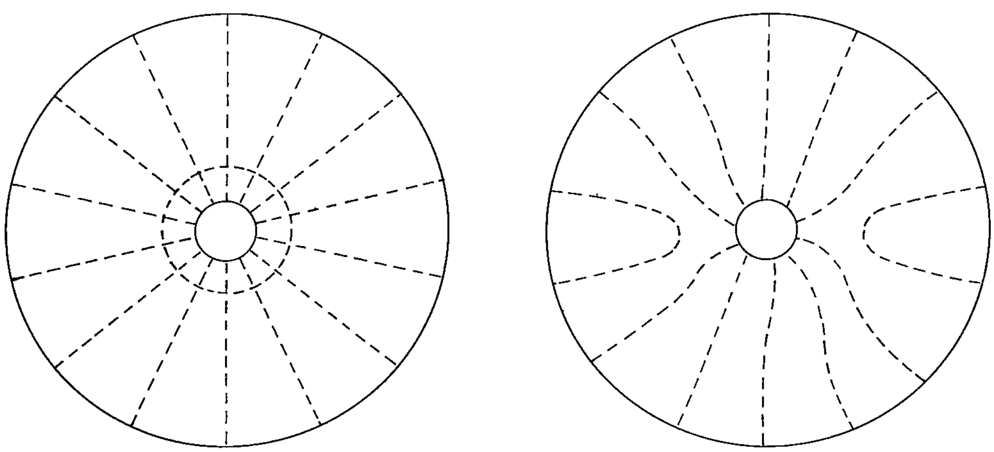

(a) Theoretical (classical). (b) Experimental (mixed).

Figure 1.- Nodal patterns of conical-frustum shells with free edges.

determined. Results were obtained for two different types of shakers. The results of the investigation are compared with frequencies and node positions calculated by means of the inextensional analysis of reference 7.

SYMBOLS

d	distance from small end of shell to the circumferential node line
f_E	frequency of the lowest frequency elastic mode
f_R	frequency of the rigid-body vertical-translation mode
l	length of shell meridian
m	longitudinal mode number (fig. 4)
n	number of circumferential waves
s	distance along cone meridian, from small end of the shell
t	thickness of shell wall
θ	angular coordinate

EXPERIMENTAL APPARATUS AND TEST PROCEDURE

Shell Models

The geometric parameters of the five conical-frustum shells tested are presented in figure 2. Typical material properties of the stainless steel used are:

Young's modulus . . . . 19.3×10^6 N/cm^2 $(28.0 \times 10^6$ lb/in$^2)$
Density . . . . 8.03 g/cm^3 (0.290 lb/in^3)

Shells 1, 2, and 3 were each constructed with a butt-welded seam. The excess material at the weld was removed so that the thickness did not vary appreciably across the weld. These shells are referred to as having "finished" seams. Shells 4 and 5 had continuous-weld lap seams along a meridian. The seam of shell 4 had 0.864 cm (0.35 inch) of overlapping material, and each of the three seams of shell 5 overlapped 0.559 cm (0.22 inch). The three seams were evenly spaced around the circumference.

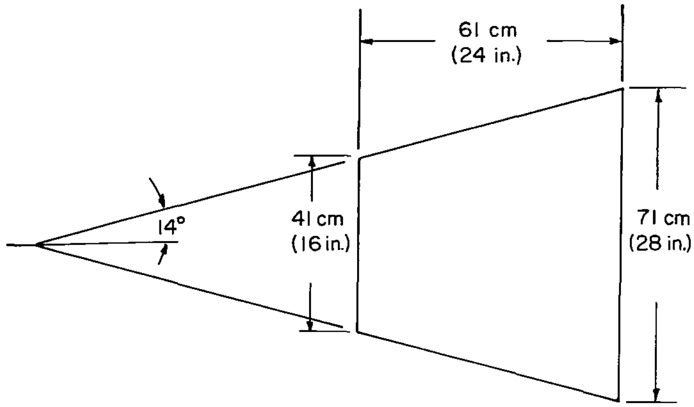

Shell	Thickness, t		Seams
	cm	in.	
1	0.0813	0.0320	Finished
2	.0432	.0170	Finished
3	.0216	.0085	Finished
4	.0445	.0175	One lap-welded
5	.0221	.0087	Three lap-welded

Figure 2.- Geometric parameters of conical-frustum shells tested.

Instrumentation

The shells were vibrated by either an air-jet shaker such as described in reference 8, or small electromagnetic shakers having a maximum force output of 6.67 newtons (1.5 lb). The air-jet shaker is advantageous in that there is no mechanical attachment to the shell. The added mass and stiffness are thus minimized, and the shaker force can be applied at various locations on the shell. The air-jet shaker had a direct-reading indicator which showed the frequency of the force.

The electromagnetic shaker was attached to the edge of the shell and had some mass and stiffness effect on the shell. Motion of the shell normal to its surface was measured by means of inductance pickups. The output of the pickup varies with its distance from the shell, and therefore no mechanical attachment was required. The pickup output was displayed on an oscilloscope, and its frequency was obtained from a direct-reading frequency meter.

Test Setup and Procedure

A typical test setup is shown in figure 3. The shells were positioned with the larger diameter upward, and the supports were attached to the upper edge. As shown in the photograph, elastic bands were introduced between the shell and the support strings to allow vertical freedom of motion of the shell at the support attachment point. The suspension stiffness was altered by using various numbers of supporting strings and various numbers of elastic bands at each support point. The frequency of the rigid-body vertical-translation mode was used as an indication of the relative stiffness of each suspension configuration. This frequency was obtained by exciting the mode manually and timing a number of cycles with a stopwatch.

Resonant frequency was determined by varying the frequency of the shaker force until the output of the pickup, as observed on the oscilloscope, was a maximum. The frequency was then read either from the air-shaker dial, the dial of the oscillator driving the electromagnetic shaker, or the direct-reading frequency meter using the pickup

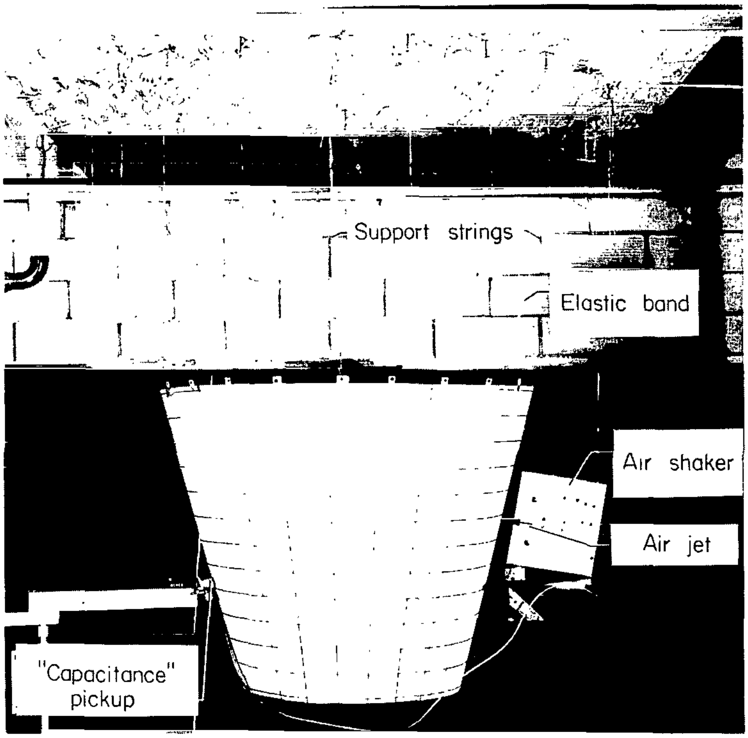

Figure 3.- Typical test setup. L-67-8726

output. Nodal patterns were then identified either by visually observing the locations of zero normal motion by means of the gridwork painted on the shell or by observing phase relations on an oscilloscope between a stationary capacitance pickup, such as shown in figure 3, and another capacitance pickup moved over the surface of the shell. Shell 2 was vibrated before and after the white background and black gridwork were painted on, and the paint was found to have a negligible effect on the resonant frequencies.

RESULTS AND DISCUSSION

In this section the general characteristics of the vibrations of a conical-frustum shell with free edges are discussed first. It is then shown that superposition of analytically obtained modes yields nodal patterns that are similar to the experimentally obtained mixed modes. Finally, the specific effects of lap-welded seams, suspension stiffness, and type of shaker on the resonant frequencies and nodal patterns are discussed.

General Characteristics

The resonant frequencies and mode data of the five conical-frustum shells are presented in table I. The frequency for a given combination of m and n is seen to be proportional to the shell thickness.

Some features of the vibration characteristics are similar for all the shells. To illustrate these features, the frequencies for shell 1 are presented in figure 4. At each value of n, the number of circumferential waves, there are two resonant frequencies in the frequency range shown. The types of mode obtained are shown in the sketches on the right-hand side of figure 4. The lowest frequency mode, designated $m = 0$, has a circular node line near the small end of the shell, while the next higher frequency mode, designated $m = 1$, has a circular node line nearer the large end. For the $m = 0$ modes the

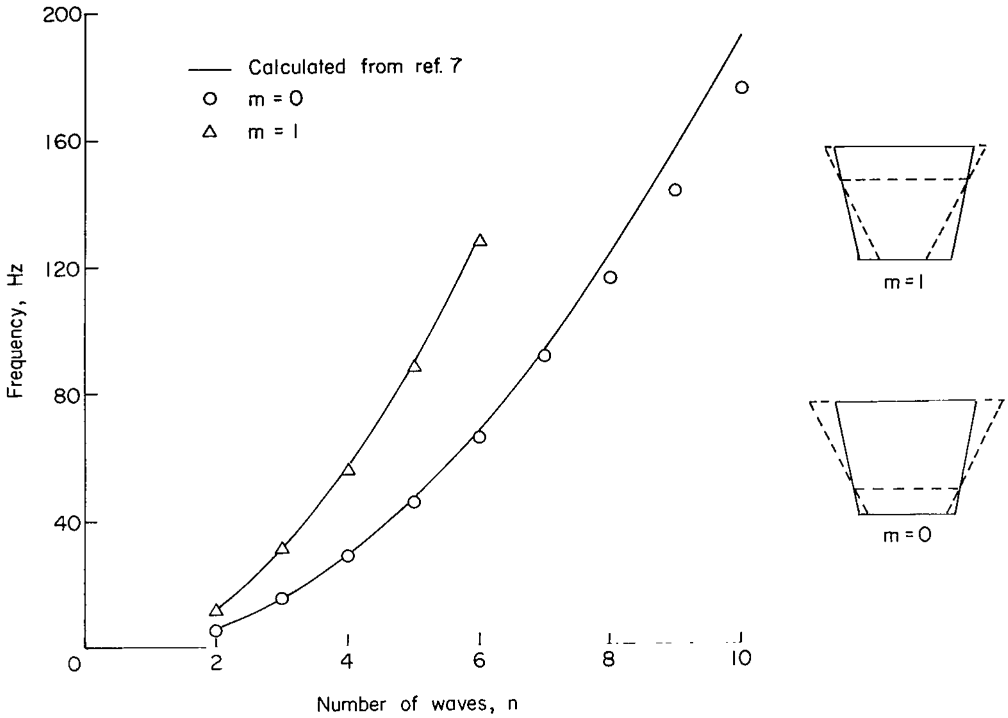

Figure 4.- Vibration characteristics of shell 1; $t = 0.0813$ cm (0.032 in.); finished seam; $f_R/f_E = 0.260$.

amplitudes are greater at the large end of the shell, while the $m = 1$ modes have greater amplitudes near the small end. The frequencies always increase with increasing values of n for each value of m (in this frequency range). In this respect the frequency curves resemble those of free-free cylinders shown in reference 1. The modes associated with all the resonant frequencies shown in figure 4 were classical modes (they had the same number of waves on both ends of the cone); therefore, these node pattern results agree with linear thin-shell theory.

Frequencies calculated by using the inextensional analyses of reference 7 are shown in figure 4 to be in good agreement with experimental frequencies at small values of n. As the value of n increases, however, the calculated frequencies become higher than the experimental frequencies. This effect supports the results of reference 7, where it is shown that a free-free cone vibrates nearly inextensionally at small n, but at large n values the middle surface apparently stretches.

The distance of the nodal circle from the small end of the shell is presented in figure 5 as a function of n for the $m = 0$ and $m = 1$ modes. The experimental data in figure 5 were obtained from the classical modes of shells 1, 2, 4, and 5. While there is some scatter in the experimental data, the agreement with the calculated values is generally good. It can be concluded from figures 4 and 5 that inextensional theory is adequate for small values of n.

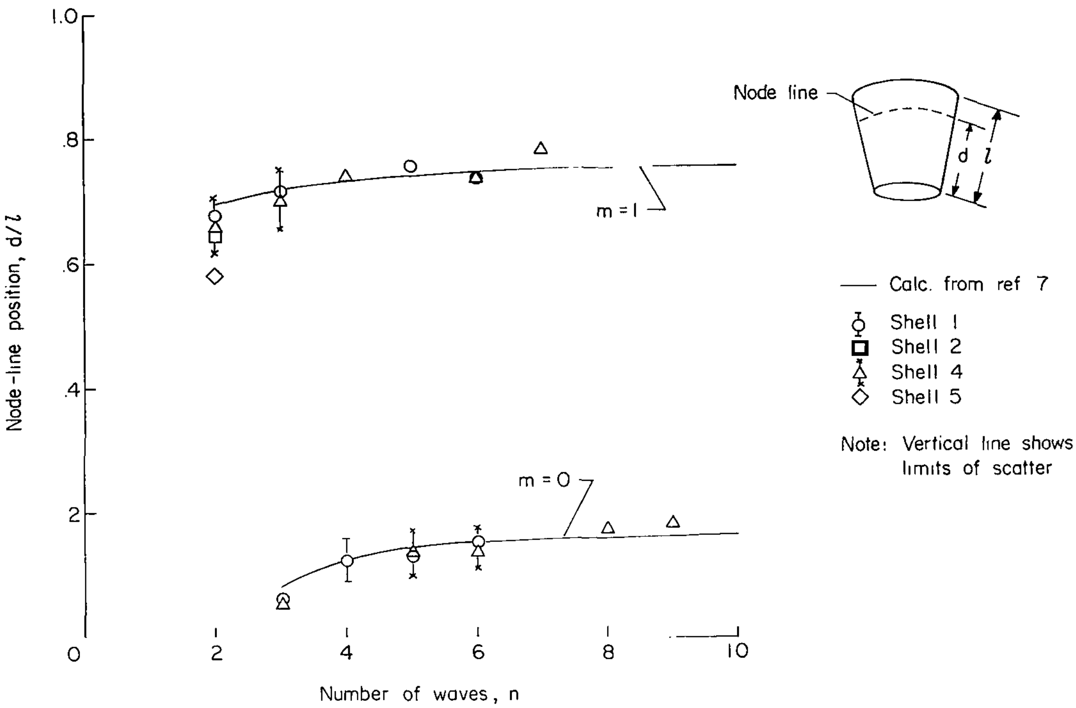

Figure 5.- Location of circle node along cone meridian.

Modal Superposition

The vibration characteristics of shells 2 and 3, the two thinner walled, finished-seam shells, are shown in figure 6. The calculated frequencies are in good agreement with experimental frequencies at small n values, but are higher at the larger n values. These results are similar to those shown in figure 4 for the shell with the thickest wall, and are also similar to the results for the shells with lap-seams, shown in later figures. Figure 6(a) shows that shell 2 (0.0432 cm thick, finished seams) has classical modes at all frequencies identified, but figure 6(b) shows that shell 3 (0.0216 cm thick, finished seams) had two mixed modes. There was an $m = 1$ mode at nearly the same frequency as each of the mixed $m = 0$ modes. This observation suggested that the mixed modes were made up of superposed classical modes coupled by some characteristics of the shell or the experimental setup.

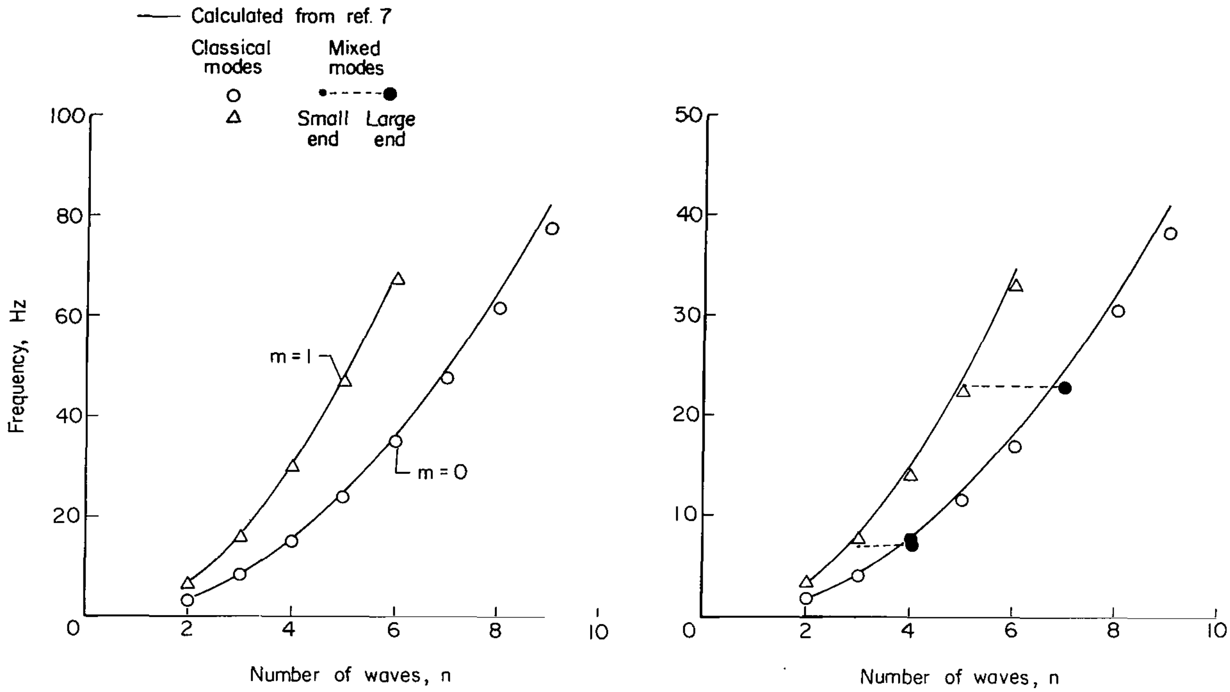

(a) Shell 2; t = 0.0432 cm (0.0170 in.); f_R/f_E = 0.334.

(b) Shell 3; t = 0.0216 cm (0.0085 in.); f_R/f_E = 0.403.

Figure 6.- Vibration characteristics of conical-frustum shells with finished seams.

In order to determine whether the experimentally observed mixed nodal patterns could be explained this way, some analytically obtained modes were superposed. The resulting nodal patterns are compared with experiment in figure 7. The experiments suggested that the $n = 3$ mode was coupling with $n = 4$ and that $n = 5$ was coupling with $n = 7$, so these components were superposed. The analysis of reference 7 indicated that the meridional mode shape predicted by inextensional theory, a straight line, was adequate for these small n values, so the straight line was used with the location of the meridional node for each mode taken from figure 5. The proportion of each mode in the superposition was chosen to make one calculated node point coincide with a corresponding experimental node point. Comparison of the experiment nodal patterns in figure 7 with the superposed patterns indicates good agreement. It can be concluded, therefore, that the mixed modes can be interpreted for these cases as superpositions of classical modes. Possible causes of coupling of classical modes include the suspension system, the method of vibrating the shells, and the presence of seams.

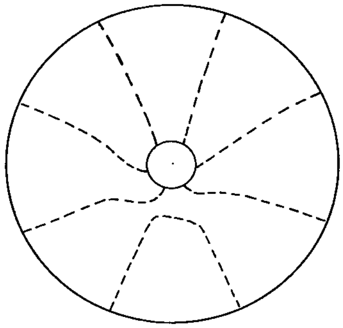

(a) Experimental, $n = 4$.

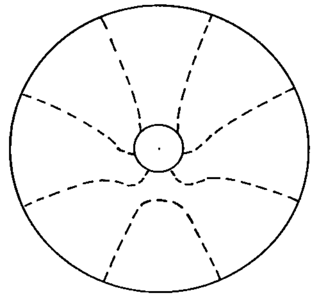

(b) Superposed,
$(s - 3)\cos 4\theta + 0.2(s - 17.8)\cos 3\theta = 0$.

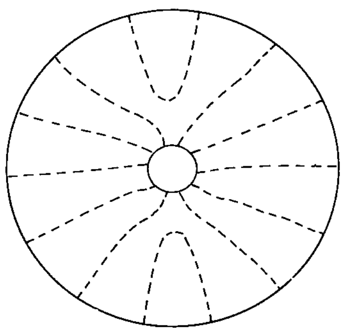

(c) Experimental, $n = 7$.

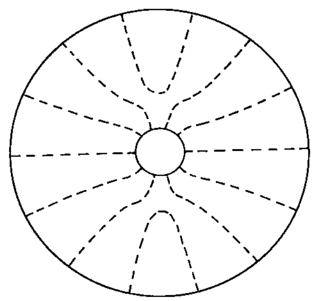

(d) Superposed,
$(s - 4)\cos 7\theta + 0.3(s - 18.8)\cos 5\theta = 0$.

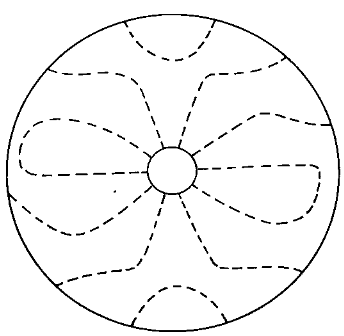

(e) Experimental, $n = 5$.

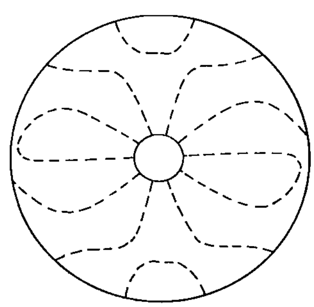

(f) Superposed,
$(s - 4)\cos 7\theta - 0.11(s - 4)\sin 7\theta + 5.2(s - 18.8)\cos 5\theta = 0$.

Figure 7.- Experimental and superposed mixed nodal patterns.

Effects of Seams

The resonant frequencies of the two shells with lap-welded seams are shown in figure 8. The relation between the experimental frequencies and the calculated frequencies is the same for these shells as for the finished-seam shells, indicating that the seams have not caused any major changes in the frequency spectrum. Shell 4, with one seam (fig. 8(a)), has one mixed mode, whereas shell 2, with one finished seam (fig. 6(a)), had none, although it had the same shell thickness and suspension stiffness. This result indicates that lap-welded seams along a meridian can cause coupling of classical modes and result in mixed modes.

Figure 8(b) shows that shell 5 has many mixed modes, whereas shell 3 (fig. 6(b)) had but two mixed modes. However, in addition to the seams, shell 5 had a number of local wrinkles, whereas shell 4 had virtually none. Because of the extreme flexibility and the free edges of shell 5, wrinkling during manufacture and test setup was virtually unavoidable. Some of the mixed modes were probably due to the local wrinkles and the extreme flexibility of the shell.

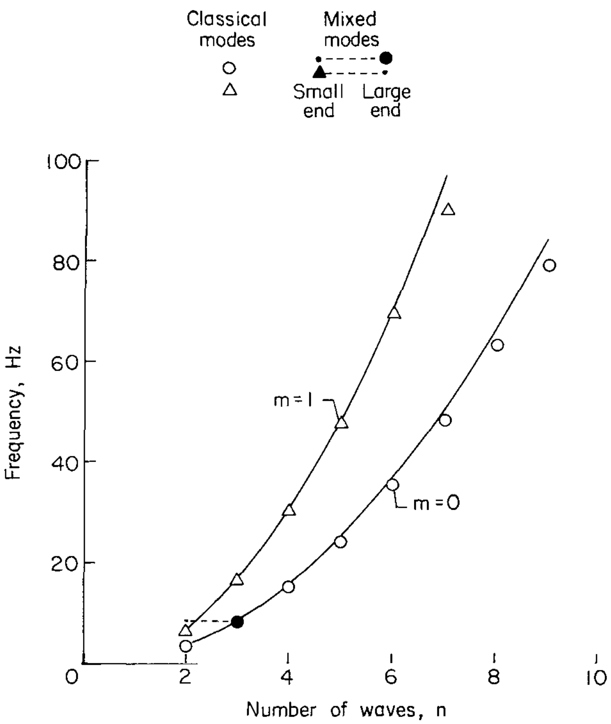

(a) Shell 4; t = 0.0445 cm (0.0175 in.); one seam; f_R/f_E = 0.334.

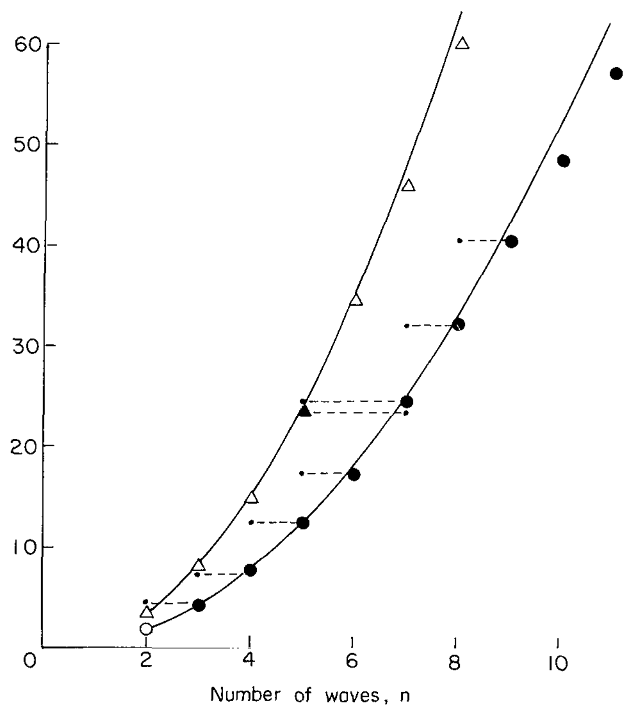

(b) Shell 5; t = 0.0221 cm (0.0087 in.); three seams; f_R/f_E = 0.408.

Figure 8.- Vibration characteristics of conical-frustum shells with lap-welded seams.

Suspension-Stiffness Effects

The effect of the suspension-system stiffness on the nodal patterns of the shells was investigated as a possible cause of the occurrence of mixed modes. The frequency of the rigid-body vertical-translation mode f_R is used as an indication of the suspension-system stiffness. The frequency f_R is divided by the frequency of the lowest frequency elastic mode ($m = 0$, $n = 2$) to obtain a number that indicates the relative stiffness of the suspension. Presumably, shells with different elastic-mode frequencies have the same suspension effects if the ratio f_R/f_E is the same. It is desirable to keep the ratio f_R/f_E as small as possible to avoid suspension-system coupling with the elastic modes. The frequencies shown in figures 4 and 6 were obtained with the smallest suspension ratios obtainable for each shell. The values of the suspension ratio for these finished-seam shells are given in the following table:

Shell	Thickness, t, cm	f_R/f_E
1	0.0813	0.260
2	.0432	.334
3	.0216	.403

This table shows that shell 3, which had two mixed modes (fig. 6(b)), had a stiffer suspension system than shells 1 and 2, which had no mixed modes (figs. 4 and 6(a)). To investigate the effect of stiffening the suspension system, shell 2 was vibrated with its suspension ratio increased to $f_R/f_E = 0.470$. The resonant frequencies were not appreciably changed by this increase; however, the $n = 4$, $m = 0$ mode became mixed. This result indicates that the suspension system causes the occurrence of mixed modes.

The progressive distortion of the $n = 4$, $m = 0$ mode as the suspension system is stiffened is shown in figure 9. The nodal pattern for $f_R/f_E = 0$ was drawn from theoretical considerations. The nodal pattern for $f_R/f_E = 0.334$ (on the upper right-hand side of the figure) shows that even though there are eight node lines on both ends of the shell, there is considerable distortion as compared with the theoretical pattern. Increasing the suspension stiffness to $f_R/f_E = 0.470$ results in such distortion of the nodal pattern that the number of nodes is different on the two ends of the shell. Finally, with the elastic bands removed from the suspension, the rigid-body plunging mode is effectively eliminated, there is no elastic "give" in the suspension strings, and the suspension ratio is $f_R/f_E = \infty$ (the value used in ref. 1). In this case only four of the node lines reach the small end of the shell. These results indicate that the character of the suspension used in the vibration testing can have a large effect on the nodal patterns obtained.

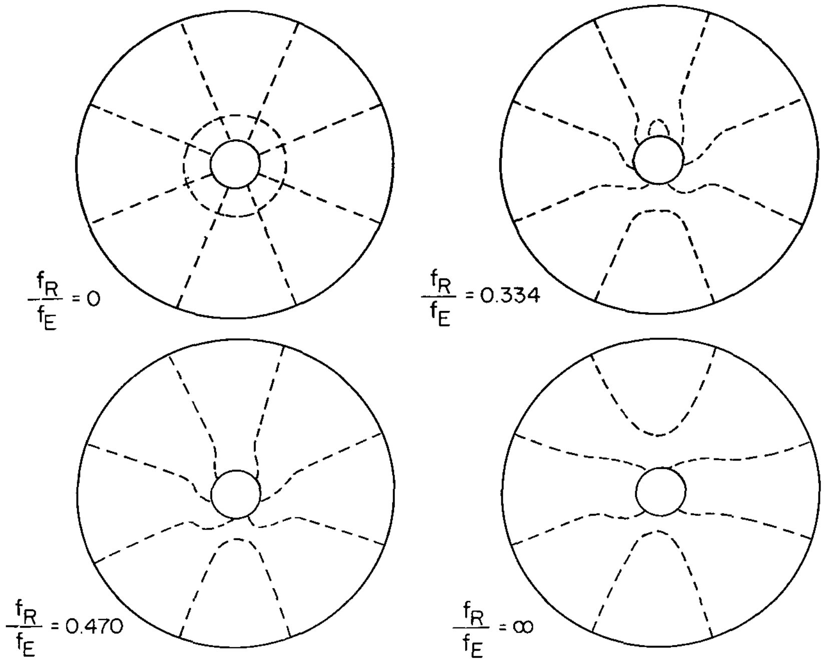

Figure 9.- Variation of nodal pattern with suspension stiffness; $t = 0.0432$ cm (0.017 in.); finished seam; $m = 0$; $n = 4$; $f = 15.0$ Hz.

Shaker Effects

The shaker location was found to cause mixed modes in some cases. For example, the $n = 4$, $m = 0$ mode was found to be sensitive to the location of the point of application of the air-shaker force. With the air shaker at the large end of the shell, this mode was mixed, with three waves at the small end of the shell, suggesting that the $n = 3$, $m = 1$ mode was responding at the same time. In order to uncouple the response the following procedure was used. First, the $n = 3$, $m = 1$ mode was tuned in by varying the shaker frequency until maximum response was obtained. Then the air shaker was moved along the meridian to the node of this mode to minimize the response. Finally, with the air shaker in this new position, the frequency was changed and the $n = 4$, $m = 0$ mode was tuned in. This mode was then found to have the same number of waves on both ends of the shell. This result indicates that the location of the shaker can cause mixed modes; however, the $n = 4$, $m = 0$ mode was the only one found to be sensitive to shaker location. The shaker position was varied in an attempt to eliminate mixed modes on other shells, but this effort was unsuccessful.

Small electromagnetic shakers having a maximum force of 6.67 newtons (1.5 lb) are frequently used (as they were in ref. 1) in testing small vibration models; therefore, it was considered to be of interest to investigate the vibrations of the thin-wall shells of these tests with such electromagnetic shakers. In figure 10 resonant frequencies

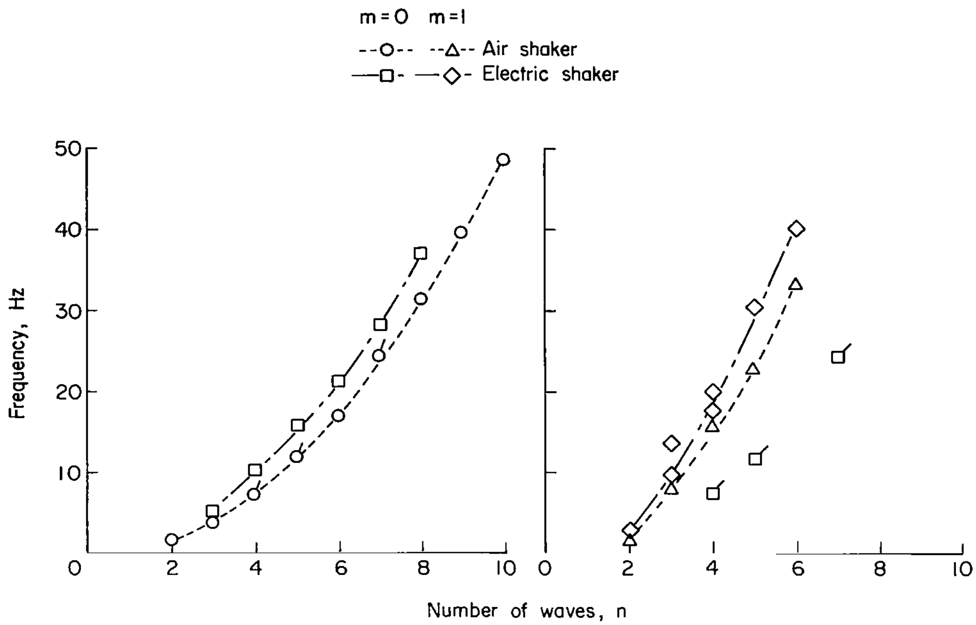

(a) Shaker on large end. (b) Shaker on small end.

Figure 10.- Vibration characteristics with air shaker and electromagnetic shakers. Shell 5; t = 0.0221 cm (0.0087 in.); three lap-welded seams; $f_R/f_E = \infty$. Flagged symbols indicate modes which responded at the same frequency when excited by either shaker.

obtained with the electromagnetic shaker are compared with those obtained with the air shaker. Figure 10(a) shows that when the shaker force was applied at the large end of the shell the only modes that responded were $m = 0$ modes, that is, modes with greater amplitudes at the large end of the shell. The resonant frequencies obtained with the electric shaker were higher, by as much as 39 percent, than those obtained with the air shaker. Figure 10(b) shows that when the air-shaker force was applied at the small end of the shell the only modes that responded were $m = 1$ modes, modes with greater amplitudes at the small end of the shell. When the electric shaker was attached at the small end of the shell, most of the modes that responded were $m = 1$ modes. These modes had higher frequencies when excited by the electric shaker than when excited by the air shaker. Some $m = 0$ modes also responded, however, and these modes had approximately the same frequency when excited by the electric shaker as when excited by the air shaker. This effect can be seen by comparing the flagged symbols in parts (a) and (b) of figure 10.

It can be concluded from figure 10 that the mass and stiffness of this particular type of electromagnetic shaker caused significant changes in the frequency characteristics of the thin-walled shells tested. Many of the modes associated with the frequencies shown in figure 10 were mixed modes; however, the frequency changes were considered to be more significant, and therefore no conclusions have been drawn regarding coupling. It should be noted that other testing techniques such as impedance methods might be used to obtain satisfactory results with the electric shakers.

SUMMARY OF RESULTS

An experimental investigation of the vibration characteristics of five conical-frustum shells with free ends has been conducted, and the results are reported herein. The effects of wall thickness, seams, suspension-system stiffness, and the type of excitation on the frequencies and nodal patterns were investigated.

In the frequency range covered, the vibration response consisted of a number of closely spaced resonant frequencies having mode shapes of two types. The mode associated with the lowest frequency at each value of n (the number of circumferential waves) had greater amplitudes at the large end of the shell and a nodal circle near the small end, while the mode associated with the next higher frequency had greater amplitudes at the small end of the shell and a nodal circle nearer the large end. The frequency for a given mode was proportional to the shell thickness.

When the finished-seam shells with thicknesses of 0.0813 cm (0.032 in.) and 0.0432 cm (0.017 in.) were tested with the air shaker and a soft suspension system, all the modes were classical modes; that is, they had the same value of n on both ends of the cone. The presence of seams or increases in suspension-system stiffness were found to be associated with an increase in the number of mixed modes, but the resonant frequencies were not changed significantly. The air-shaker location and increased suspension stiffness appeared to cause coupling of modes having another mode at nearly the same frequency, but seams (and other imperfections associated with the thinnest shell) caused modes to be coupled when no other mode was nearby. The apparent resonant frequencies obtained with the electromagnetic shakers varied considerably from those obtained with the air shaker.

The resonant frequencies and meridional node position were calculated by using inextensional theory and were found to be in good agreement with experimental values for the smaller values of n. The fact that the experimentally observed nodal patterns of the mixed modes could be obtained by superposition of calculated modes suggests that the mixed modes were caused by some physical characteristic of the shell or experimental setup that caused coupling of classical modes.

Langley Research Center,
National Aeronautics and Space Administration,
Langley Station, Hampton, Va., October 26, 1967,
124-08-05-08-23.

REFERENCES

1. Watkins, Jerry D.; and Clary, Robert R.: Vibrational Characteristics of Some Thin-Walled Cylindrical and Conical Frustum Shells. NASA TN D-2729, 1965.
2. Weingarten, V. I.: Free Vibrations of Conical Shells. Proc. Am. Soc. Civil Engrs., J. Eng. Mech. Div., vol. 91, no. EM4, Aug. 1965, pp. 69-87.
3. Tang, Chao-tsein; and Hong, Zhong-yu: The Vibration Behavior of Circular Conical Shells. Acta Mech. Sinica, vol. 9, no. 1, Jan./Mar. 1966, pp. 15-26.
4. Koval, Leslie R.: Note on the Vibrational Characteristics of Thin-Walled Shells. AIAA J. (Tech. Comments), vol. 4, no. 3, Mar. 1966, pp. 571-572.
5. Novozhilov, V. V. (P. G. Lowe, trans.): The Theory of Thin Shells. P. Noordhoff Ltd. (Groningen, The Netherlands), 1959, p. 304.
6. Hu, William C. L.: Comments on "Vibrational Characteristics of Thin-Wall Conical Frustum Shells." AIAA J. (Tech. Comments), vol. 3, no. 6, June 1965, p. 1213.
7. Hu, W. C. L.; Gormley, J. F.; and Lindholm, U. S.: An Experimental Study and Inextensional Analysis of Vibrations of Free-Free Conical Shells. Intern. J. Mech. Sci., vol. 9, Mar. 1967, pp. 123-135.
8. Herr, Robert W.: A Wide-Frequency-Range Air-Jet Shaker. NACA TN 4060, 1957.

TABLE I.- RESONANT FREQUENCIES OF CONICAL-FRUSTUM SHELLS WITH FREE ENDS

m	n	Shell 1, t = 0.0813 cm (0.032 in.), finished seam		Shell 2[a], t = 0.0432 cm (0.017 in.), finished seam		Shell 3, t = 0.0216 cm (0.0085 in.), finished seam		Shell 4, t = 0.0445 cm (0.0175 in.), one lap seam		Shell 5, t = 0.0221 cm (0.0087 in.), three lap seams	
		Frequency, Hz	Mode[b]	Frequency, Hz	Mode[b]	Frequency, Hz	Mode[b]	Frequency, Hz	Mode[b]	Frequency, Hz	Mode[b]
Rigid-body modes	0	1.52		1.1		0.725		1.1		0.775	
	1	1.75		1.7		1.4		1.7		1.5	
0	2	5.85		3.3		1.8		3.3		1.9	
	3	15.45		8.3		4.0		8.4	3-2	4.2	3-2
	4	28.6		15.0		7.2/7.55	4-3	15.35		7.7	4-3
	5	45.5		24.0		11.55		24.5		12.5	5-4
	6	65.9		35.0		17.0		35.8		17.4	6-5
	7	91.0		47.6		22.8	7-5	48.7		24.5	7-5
	8	115.5		61.7		30.6		63.5		32.2	8-7
	9	143.0		77.5		38.3		79.2		40.5	9-8
	10	175.0		----		---------		-----		48.5	
	11	------		----		---------		-----		57.2	
1	2	11.9		6.2		3.35		6.3		3.5	
	3	30.6		15.7		7.6		16.2		8.0	
	4	55.4		29.5		14.0		30.4		14.7	
	5	87.5		46.6		22.4		47.8		23.5	7-5
	6	127.0		67.1		32.9		69.3		34.5	
	7	------		----		---------		90.0		45.9	
	8	------		----		---------		-----		60.0	

[a]Shell 2 was also tested with the suspension stiffened so that the frequencies of the rigid-body modes were 1.55 Hz for $n = 0$ and 2.0 Hz for $n = 1$. The elastic frequencies were not changed from those shown, but the $m = 0$, $n = 4$ mode was mixed, 4-3.

[b]No entry for classical modes. For mixed modes, first digit is number of waves on large end and second digit is number of waves on small end of shell.

National Aeronautics and Space Administration
WASHINGTON, D. C.

OFFICIAL BUSINESS

FIRST CLASS MAIL

POSTAGE AND FEES PAID
NATIONAL AERONAUTICS AND
SPACE ADMINISTRATION

080 001 57 51 3DS 68074 00903
AIR FORCE WEAPONS LABORATORY/AFWL/
KIRTLAND AIR FORCE BASE, NEW MEXICO 87117

[illegible] CHIEF TECH. [illegible]
[illegible]

POSTMASTER: If Undeliverable (Section 158 Postal Manual) Do Not Return

"The aeronautical and space activities of the United States shall be conducted so as to contribute . . . to the expansion of human knowledge of phenomena in the atmosphere and space. The Administration shall provide for the widest practicable and appropriate dissemination of information concerning its activities and the results thereof."

—NATIONAL AERONAUTICS AND SPACE ACT OF 1958

NASA SCIENTIFIC AND TECHNICAL PUBLICATIONS

TECHNICAL REPORTS: Scientific and technical information considered important, complete, and a lasting contribution to existing knowledge.

TECHNICAL NOTES: Information less broad in scope but nevertheless of importance as a contribution to existing knowledge.

TECHNICAL MEMORANDUMS: Information receiving limited distribution because of preliminary data, security classification, or other reasons.

CONTRACTOR REPORTS: Scientific and technical information generated under a NASA contract or grant and considered an important contribution to existing knowledge.

TECHNICAL TRANSLATIONS: Information published in a foreign language considered to merit NASA distribution in English.

SPECIAL PUBLICATIONS: Information derived from or of value to NASA activities. Publications include conference proceedings, monographs, data compilations, handbooks, sourcebooks, and special bibliographies.

TECHNOLOGY UTILIZATION PUBLICATIONS: Information on technology used by NASA that may be of particular interest in commercial and other non-aerospace applications. Publications include Tech Briefs, Technology Utilization Reports and Notes, and Technology Surveys.

Details on the availability of these publications may be obtained from:

SCIENTIFIC AND TECHNICAL INFORMATION DIVISION

NATIONAL AERONAUTICS AND SPACE ADMINISTRATION

Washington, D.C. 20546